IS BOUNCE JUGGLING EASIER IN A PARABOLIC BILLIARD THAN IN A WEDGE?

Dong Eui Chang
Electrical Engineering and Computer Science
University of Liège
B-4000 Liège, Belgium
chang@montefiore.ulg.ac.be

Renaud Ronsse
Electrical Engineering and Computer Science
University of Liège
B-4000 Liège, Belgium
R.Ronsse@ulg.ac.be

Rodolphe Sepulchre
Electrical Engineering and Computer Science
University of Liège
B-4000 Liège, Belgium
r.sepulchre@ulg.ac.be

Abstract

We study the dynamics and control of bounce juggling in two planar gravitational billiards: a wedge, parameterized by its angle, and a parabola, parameterized by its curvature. The two elastic and unactuated (fixed) billiards possess the same period-one and period-two orbits. Some of them are shown to be unstable in the wedge, whereas all of them are shown to be marginally stable in the parabola, due to an additional conserved quantity. We discuss implications of this result for the control problem of juggling these orbits in an actuated nonelastic billiard.

Key words

Billiard, juggling, feedback, sensorless, stabilization

1 Introduction

Bounce juggling is an interesting control problem that has been investigated by several researchers as a benchmark for intermittent control of impact systems; see, for example, [Buehler, Koditschek and Kindlmann, 1994; Lynch and Black, 1999; Brogliato, 1996; Schaal and Atkeson, 1993; Sepulchre and Gerard, 2003; Ronsse, Lefevre and Sepulchre, 2004] and references therein. In recent papers [Sepulchre and Gerard, 2003; Gerard and Sepulchre, 2004; Ronsse, Lefevre and Sepulchre, 2004], we studied the stabilization of period-one and period-two periodic orbits in a wedge; see Figure 1. Period-two (see (a) of Figure 2) orbits resemble the classical "shower" juggling pattern and allow to consider the bounce juggling control of several balls.

A dynamical study of the elastic unactuated (fixed) wedge shows that period-one orbits exist for all angle θ. They are marginally stable for $\theta < 45^\circ$, exponentially unstable for $\theta > 45^\circ$, and just unstable – not exponentially unstable – for $\theta = 45^\circ$. In contrast, period-two orbits exist only in the square wedge ($\theta = 45^\circ$). There is a continuum of such orbits in the square wedge and they are all unstable. Feedback strategies [Gerard and Sepulchre, 2004] as well as sensorless strategies [Ronsse, Lefevre and Sepulchre, 2004] were investigated to stabilize these orbits in a nonelastic but moving wedge.

In the present paper, we further investigate the role of the billiard shape in this control problem. We study the dynamics of a parabolic billiard first studied in [Korsch and Lang, 1991]. The parabolic billiard is parameterized by its curvature, whereas the wedge billiard is parameterized by its angle. Compared to the wedge, the parabolic billiard has an additional conserved quantity and we examine its consequences for the bounce juggling control problem. We derive a reduced Poincaré map for the parabolic billiard and study the existence and stability of some families of periodic orbits. In particular, we show that the same period-one and period-two orbits exist in both billiards but that these orbits are always marginally stable in the parabolic billiard.

The stabilizing role of the parabolic shape can be exploited in the bounce juggling control problem. For instance, in [Gerard and Sepulchre, 2004], a simple feedback control strategy was proposed to exponentially stabilize orbits that are marginally stable in the elastic wedge. This strategy was restricted to period-one orbits and to $\theta < 45^\circ$ in the wedge. In contrast, we show that it is applicable to period-one orbits in the parabolic billiard.

The paper is organized as follows: Section 2 reviews the main properties of the wedge billiard dynamics. Section 3 reviews the derivation of the parabolic billiard dynamics and proposes a bifurcation analysis of some families or orbits based on the analytical derivation of a reduced Poincaré map. Section 4 compares the analysis of both billiards and discusses its implications for the control of bounce juggling.

2 Review of the Wedge Dynamics

We review the analysis the wedge dynamics from [Lehtihet and Miller, 1986; Ronsse, Lefevre and Sepulchre, 2004; Sepulchre and Gerard, 2003]; see Figure 1 for the wedge billiard. For any $\theta \in (0°, 90°)$, there always exist periodic orbits with the shape of a single arch; see (a) of Figure 2. For convenience, we call them *period-one* orbits. Only when $\theta = 45°$, namely, for the square wedge, there exist periodic orbits with the shape of a double arch; see (b) of Figure 2. They are called *period-two* orbits for convenience.

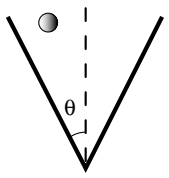

Figure 1. The wedge.

Period-one orbits are marginally stable for $\theta < 45°$ because the three different eigenvalues of the Poincaré map have magnitude 1. Moreover, the phase portrait of the Poincaré map has integral, KAM and chaotic regions for $\theta < 45°$. Period-one orbits are unstable for $\theta = 45°$. Period-one orbits are exponentially unstable for $\theta > 45°$ because one of the eigenvalue of the Poincaré map has magnitude greater than 1. Moreover, all the periodic orbits are known to be unstable and the wedge dynamics are chaotic for $\theta > 45°$. Period-two orbits, which exist only for the square wedge, are all unstable.

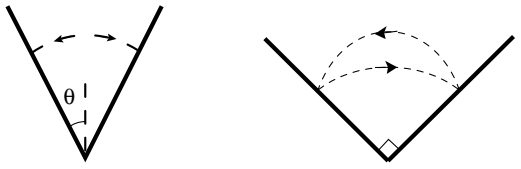

(a) A period-one orbit (b) A period-two orbit

Figure 2. Period-one orbits exist for all θ, but period-two orbits exist only for the square wedge.

3 Parabolic Gravitational Billiards

A gravitational billiard with a parabolic boundary is called a parabolic gravitational billiard (PGB). This billiard system is integrable as Hamiltonian system with two first integrals when collision is elastic , [Korsch and Lang, 1991]. In this section, we build a one-dimensional reduced Poincaré map of this system, detect some periodic orbits of the system and check their stability. In this section we assume that collision with the boundary is elastic.

3.1 Review of PGB

We review the analysis of the PGB in [Korsch and Lang, 1991] and build a three-dimensional Poincaré map.

Consider the motion of a particle of unit mass under the gravitational force with a parabolic boundary $y = \frac{1}{2}ax^2$, $a > 0$. The configuration space M is given by

$$M = \left\{ (x, y) \in \mathbb{R}^2 : y \geq \frac{1}{2}ax^2 \right\}.$$

The phase space N ($\subset T^*\mathbb{R}^2$) is given by

$$\begin{aligned} N = &\{(x, y, p_x, p_y) \in \mathbb{R}^4 : \\ &y \geq \frac{1}{2}ax^2, \neg[y = \frac{1}{2}ax^2, p_y = axp_x]\}. \end{aligned}$$

We exclude the boundary points with $p_y = axp_x$ from N because the velocity vector (p_x, p_y) is tangent to the boundary and this means that the ball is rolling on the parabola, which is out of our interest in this paper. Define the boundary B by

$$B = \left\{ (x, y, p_x, p_y) \in N : y = \frac{1}{2}ax^2 \right\}.$$

Let us define two sets of coordinates for B. Let

$$B_1 = \{(x, p_x, p_y) \in \mathbb{R}^3 : p_y \neq axp_x\}$$

and

$$B_2 = \{(x, p_t, p_n) \in \mathbb{R}^3 : p_n \neq 0\}.$$

Define $\psi_1 : B_1 \to B$ by

$$\psi_1(x, p_x, p_y) = \left(x, \frac{1}{2}ax^2, p_x, p_y \right).$$

Define $\psi_2 : B_2 \to B$ by

$$\psi_2(x, p_t, p_n) = \left(x, \frac{ax^2}{2}, \frac{p_t - axp_n}{\sqrt{1 + a^2x^2}}, \frac{axp_t + p_n}{\sqrt{1 + a^2x^2}} \right).$$

The map ψ_1 expresses vectors at the boundary in the Cartesian frame $[\mathbf{e}_x, \mathbf{e}_y]$ and the map ψ_2 in the tangent-normal moving frame $[\mathbf{e}_t, \mathbf{e}_n]$ where the two frames have the same orientations such that the vector $\mathbf{e}_n$ at the boundary of M always points to the inside of M, [Korsch and Lang, 1991].

The Hamiltonian of this system is given by

$$H = \frac{1}{2}(p_x^2 + p_y^2) + gy \tag{1}$$

where $g > 0$ is the gravitational constant. When the mass of the particle is not one, one can always rescale the time such that the Hamiltonian takes the above form with a different value of g.

We now build a Poincaré map, $\mathcal{P} : B \to B$. Since the particle starting from B with $p_n > 0$ will reach B and then rebound at the boundary, $\mathcal{P}$ can be decomposed into two maps: the flight map $\mathcal{C}$ and the bouncing map $\mathcal{B}$. The flight map $\mathcal{C}$ is given in the coordinates (x, p_x, p_y) by

$$\psi_1^{-1} \circ C \circ \psi_1(x, p_x, p_y) = \begin{pmatrix} \frac{(g-ap_x^2)x+2p_xp_y}{g+ap_x^2} \\ p_x \\ p_y - \frac{2g(p_y-axp_x)}{g+ap_x^2} \end{pmatrix}.$$

The bouncing map $\mathcal{B}$ with elastic collision is given in (x, p_t, p_n) by

$$\psi_2^{-1} \circ \mathcal{B} \circ \psi_2(x, p_t, p_n) = (x, p_t, -p_n).$$

Hence, one can easily compute the Poincaré map

$$\mathcal{P} = \mathcal{B} \circ \mathcal{C} \tag{2}$$

in terms of (x, p_x, p_y) or (x, p_t, p_n).

3.2 Reduced Poincaré Map

When collision is elastic on the boundary, the dynamics of the PGB have two first integrals: H and G, where H is the Hamiltonian in (1) and G is defined by

$$G(x, y, p_x, p_y) = xp_xp_y - \left(y - \frac{1}{2a}\right)p_x^2 + \frac{1}{2}gx^2. \tag{3}$$

See [Landau and Lifshitz, 1976] for the derivation of G with the Hamilton-Jacobi equation. Both functions are invariant under $\mathcal{C}$ and $\mathcal{B}$, i.e.,

$$H \circ \mathcal{C} = H, \quad H \circ \mathcal{B} = H,$$
$$G \circ \mathcal{C} = G, \quad G \circ \mathcal{B} = G.$$

See [Korsch and Lang, 1991] for more details. Notice that the two first integrals H and G satisfy

$$(H - aG) = \frac{1}{2}(axp_x - p_y)^2 > 0 \tag{4}$$

on N.

We give one physical interpretation of the function G. Suppose that a ball is launched at $(x, y = \frac{1}{2}ax^2)$ on the boundary with the initial momentum (p_x, p_y), $p_x \neq 0$. Its (parabolic) trajectory intersects with the y-axis, say at $(0, y_0)$ with

$$y_0 = -\frac{p_y}{p_x}x + \frac{1}{2}ax^2 - \frac{g}{2p_x^2}x^2, \tag{5}$$

forward or backward in time; see Figure 3. From (3) and (5), it follows

$$G = \left(\frac{1}{2a} - y_0\right)p_x^2.$$

Since $(x, y) = (0, \frac{1}{2a})$ is the focal point of the parabola $y = \frac{1}{2}ax^2$, one can interpret G as the signed distance from y_0 to the focal point scaled by p_x^2 (notice that p_x is also constant in time between collisions).

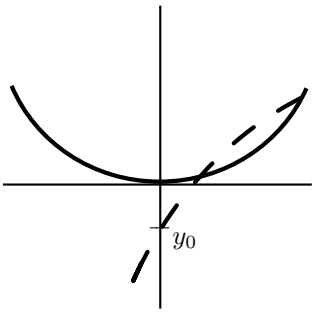

Figure 3. Each non-degenerate parabolic trajectory intersects with the y-axis in the absence of any boundaries.

As we have two first integrals, we can construct an one-dimensional reduced Poincaré map by restricting the Poincaré map $\mathcal{P}$ in (2) to a fixed level set of (H, G). Let $\mathcal{P}_{H,G}$ denote the reduced Poincaré map. Its domain will be constructed below. A simple algebra yields

$$\mathcal{P}_{H,G}(x) = \frac{2aG - Q(x)}{ax(g + aQ(x))} \tag{6}$$

where $Q(x)$ is a non-negative real root of the following quadratic equation in Q:

$$\begin{aligned}&(1 + a^2x^2)^2Q^2 \\ &+ 2a(ga^2x^4 + (2a^2G - 4aH + g)x^2 - 2G)Q \\ &+ a^2(gx^2 - 2G)^2 = 0.\end{aligned} \tag{7}$$

Since the numerator $(2aG - Q(x))$ has a factor x, the reduced Poincaré map, $\mathcal{P}_{H,G}$ is well-defined. The do-

main $B_{H,G}$ of $\mathcal{P}_{H,G}$ is given by the set of x satisfying

$$(ga^2x^4 + (g - 2aH)x^2 - 2G) \leq 0, \quad (8)$$
$$ga^2x^4 + (2a^2G - 4aH + g)x^2 - 2G \leq 0 \quad (9)$$

where the first inequality comes from the roots of (7) being real and the second from the roots of (7) being both non-negative.

One can check that the root $Q(x)$ is the same as p_x^2 at the collision point x. As there are always two non-negative roots of (7) for $x \in B_{H,G}$, one of the two is the pre-collision p_x^2 and the other the post-collision p_x^2. Let Q_b and Q_s be the bigger and the smaller root, respectively, of the quadratic equation (7). Notice the symmetry:

$$Q_b(x) = Q_b(-x), \quad Q_s(x) = Q_s(-x).$$

Let $\mathcal{P}^b_{H,G}$ be the Poincaré map $\mathcal{P}_{H,G}$ with $Q = Q_b$, and $\mathcal{P}^s_{H,G}$ with $Q = Q_s$. Then, one can see check

$$\mathcal{P}^s_{H,G}(x) = -\mathcal{P}^b_{H,G}(-x). \quad (10)$$

We give the choice rule of Q_b and Q_s:

IF $Q_b(x_{i+1}) == Q(x_i)$
  $Q(x_{i+1}) := Q_s(x_{i+1})$
ELSE
  $Q(x_{i+1}) := Q_b(x_{i+1})$
END

where $x_{i+1} = \mathcal{P}_{H,G}(x_i)$. This rule comes from the assumption of energy conservation and elastic collision.

3.3 Periodic Orbits

We find four different types of periodic orbits in the PGB dynamics using the reduced Poincaré map, and discuss their stability in the reduced space, i.e., on the level set of (H, G).

Vertical Bouncing. Suppose there is x such that $\mathcal{P}_{H,G}(x) = x$. Solve (6) for Q – i.e., $Q = a(2G - gx^2)/(1 + a^2x^2)$ – and plug it into (7) to get

$$x^2(2G - gx^2) = 0.$$

There are three roots to the above equation: $x = 0, \pm\sqrt{2G/g}$. We here deal with $x = 0$ only, postponing the analysis of $x = \pm\sqrt{2G/g}$. When does $x = 0$ become a fixed point and what about its stability? One can compute

$$\mathcal{P}_{H,G}(0) = -4\,\frac{\sqrt{a\,(H - aG)\,G}}{g + 2\,a^2G}.$$

Hence, $\mathcal{P}_{H,G}(0) = 0$ if and only if $G = 0$ since $(H - aG) > 0$. This fixed point of $\mathcal{P}_{H,G}$ corresponds to the vertical bouncing at $x = 0$.

By (8) and (9), the domain $B_{H,G}$ of the reduced Poincaré map $\mathcal{P}_{H,G}$ with $G = 0$ is given by

$$B_{H,G} = \begin{cases} \left[-\sqrt{\frac{2aH-g}{ga^2}}, \sqrt{\frac{2aH-g}{ga^2}}\right] & \text{if } (2aH - g) > 0 \\ \{0\} & \text{if } (2aH - g) \leq 0. \end{cases}$$

We now study the stability of the fixed point $x = 0$. When $(2aH - g) > 0$, one can compute

$$\mathcal{P}'_{H,G}(0) = -\left(\sqrt{\frac{2aH}{g}} + \sqrt{\frac{2aH - g}{g}}\right)^2 < -1.$$

Hence, $x = 0$ is an unstable fixed point when $(2aH - g) > 0$. On the other hand, if $(2aH - g) \leq 0$, then $x = 0$ becomes an isolated solution of $G = 0$ for each value of H satisfying $0 < H \leq \frac{g}{2a}$. In this case the vertical bouncing at $x = 0$ is Lyapunov stable even in the whole phase space N according to Theorem 1 in [Aeyels and Sepulchre, 1992].

Period-one Orbits. An orbit like the one in Figure 4 is called a period-one orbit. Let us find all period-one orbits. They satisfy

$$x \mapsto -x \mapsto x \mapsto -x \ldots. \quad (11)$$

To find these orbits, we solve $\mathcal{P}(x) = -x$ in (6) for Q:

$$(1 - a^2x^2)Q(x) = a(2G + gx^2). \quad (12)$$

If $x \neq \pm\frac{1}{a}$ (i.e., the case of $x = \pm\frac{1}{a}$ will be treated separately), one can solve (12) for $Q(x)$ and plug it into (7) to get

$$\begin{aligned} &2ga^3(H - aG)x^4 \\ &+ (g^2 + 4a^3HG + 6ga^2G - 2agH)x^2 \\ &- 4aG(H - aG) = 0. \end{aligned} \quad (13)$$

Notice that $\mathcal{P}_{H,G}(-x) = x$ and $Q(-x) = Q(x)$. Notice also that x uniquely determines $Q(x)$ by (12). Hence, by energy conservation, orbits corresponding to (12) cannot be period-two but period-one. So, we need to check $Q_b(x) = Q_s(x) = Q(x)$. That is, we need to check the compatibility of (13) and the condition of existence of the *double root* of (7), which is given by

$$ga^2x^4 + (g - 2aH)x^2 - 2G = 0. \quad (14)$$

Equations (13) and (14) are compatible, except for $x = 0$, if and only if

$$G = -\frac{1}{2g}\left(H - \frac{g}{2a}\right)^2. \quad (15)$$

Equation (15) implies that (14), as a quadratic equation in x^2, has the double root

$$x^2 = \frac{2aH - g}{2ga^2} > 0. \tag{16}$$

The corresponding Q is given by

$$Q(x) = \frac{(2aH - g)}{2a} > 0. \tag{17}$$

Notice that (15) and (17) give the condition on (H, G) for the existence of those orbits which is located at x in (16).

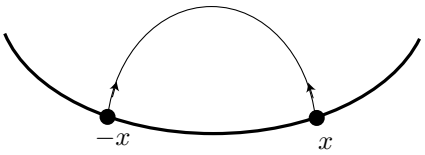

Figure 4. A period-one orbit. It satisfies $\mathcal{P}_{H,G}(\pm x) = \mp x$ and the one way of the trajectory coincides with the other way.

We now consider the case of $x = \pm\frac{1}{a}$. From (6) and (12), one can check that $\mathcal{P}_{H,G}$ is well-defined at $x = \pm\frac{1}{a}$ and it is given by

$$\mathcal{P}_{H,G}\left(\pm\frac{1}{a}\right) = \mp\frac{1}{a}.$$

The substitution of $x = \pm\frac{1}{a}$ into (12) yields

$$G = -\frac{g}{2a^2}.$$

We now choose the value of $Q(\pm\frac{1}{a})$ such that there exists a period-one orbit at $x = \pm\frac{1}{a}$. Plug $x = \pm\frac{1}{a}$ and $G = -\frac{g}{2a^2}$ into (7) and we get

$$Q^2 - \left(\frac{g}{a} - 2H\right)Q + \frac{g^2}{a^2} = 0. \tag{18}$$

The non-negative (real) roots are given by

$$Q\left(\pm\frac{1}{a}\right) = \left(H - \frac{g}{2a}\right) \pm \sqrt{\left(H - \frac{g}{2a}\right)^2 - \frac{g^2}{a^2}} \tag{19}$$

with

$$H \geq \frac{3g}{2a}.$$

It corresponds to a period-one orbit if and only if (18) has the double root if and only if

$$H = \frac{3g}{2a}.$$

Since formulas (15) – (17) derived for $x =\neq \pm\frac{1}{a}$ hold at $x = \pm\frac{1}{a}$ as well, one can parameterize all the period-one orbits, or the positive fixed points of $\mathcal{P}_{H,G} \circ \mathcal{P}_{H,G}$, as

$$x_H = \sqrt{\frac{2aH - g}{2ga^2}}, \quad H > \frac{g}{2a}. \tag{20}$$

We now check the stability of the period-one orbits. Substituting (15) into (8) and (9), one can see that the domain of $\mathcal{P}_{H,G}$ containing $\{\pm x_H\}$ is exactly the two-point set $\{\pm x_H\}$. Hence, this period-one orbit is an isolated solution of (15). According to Theorem 1 in [Aeyels and Sepulchre, 1992], the period-one orbit is Lyapunov stable in the whole phase space, N.

Period-two Orbits. We now investigate the case where the two roots (19) of (18) are different for the periodic orbits:

$$\frac{1}{a} \mapsto -\frac{1}{a} \mapsto \frac{1}{a} \mapsto -\frac{1}{a} \ldots.$$

They are period-two orbits illustrated in Figure 5. They exist if and only if

$$H > \frac{3g}{2a}, \quad G = -\frac{g}{2a^2}. \tag{21}$$

The points $(x, y) = (\pm\frac{1}{a}, \frac{1}{2a})$ are the points on the boundary where the tangent vectors at the points to the boundary have slopes $\pm 45°$. Hence, the bifurcation of the period-two orbits from the period-one orbits at $(x, y) = (\pm\frac{1}{a}, \frac{1}{2a})$ agrees with the analysis of the wedge in that in the wedge dynamics the period one orbits exist for all values of the angle between the left arm and the right arm of the wedge and the period-two orbits occur only when the wedge is square. The stability can be checked by directly computing

$$\mathcal{P}'_{H,G}\left(\pm\frac{1}{a}\right) = 1.$$

That is, all the period-two orbits are marginally stable. This result is in the contrast with the instability of all the period-two orbits in the square wedge.

Vertical Bouncing + Period-one Orbits. Recall that in searching for fixed points of $\mathcal{P}_{H,G}$ we found candidates

$$x_\pm = \pm\sqrt{\frac{2G}{g}}, \quad G > 0. \tag{22}$$

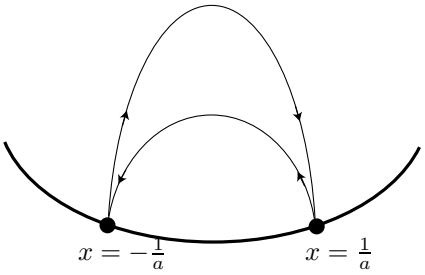

Figure 5. A period-two orbit. It satisfies $\mathcal{P}_{H,G}(x) = -x$ only at $x = \frac{1}{a}$ and the one way of the trajectory is different from the other way.

With $x = x_\pm$ in (7), one solves for Q:

$$Q_s = 0, \quad Q_b = \frac{16ga^2G(H - aG)}{(g + 2a^2G)^2}. \qquad (23)$$

By the choice rule of Q, it is impossible to have

$$(x_-, Q_s) \mapsto (x_-, Q_b) \mapsto (x_-, Q_s) \dots$$

or

$$(x_+, Q_s) \mapsto (x_+, Q_b) \mapsto (x_+, Q_s) \dots .$$

Namely, $x_\pm$ cannot be the fixed points of $\mathcal{P}_{H,G}$. Instead, the following is possible

$$(x_-, Q_s) \mapsto (x_-, Q_b) \mapsto (x_+, Q_s) \mapsto (x_+, Q_b) \\ \mapsto (x_-, Q_s) \mapsto \dots$$

provided the following holds

$$H = \frac{g^2 + 8ga^2G - 4a^4G^2}{4a(g - 2a^2G)}, \ 0 < G < \frac{g}{2a^2} \qquad (24)$$

where $G < \frac{g}{2a^2}$ comes from (4). The corresponding periodic orbits are illustrated in Figure 6.

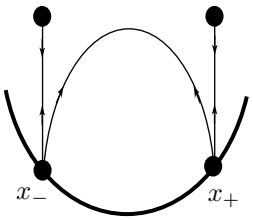

Figure 6. (Vertical bouncing + period-one) periodic orbits.

General stability analysis of the (vertical bouncing+period-one) periodic orbits is not straightforward. One needs to rely on numerical computation given specific numeric data of all parameters.

Bifurcation Diagram. We have found the four different types of periodic orbits: vertical bouncing, period-one, period-two and (vertical bouncing+period-one) orbits. We now study how they bifurcate from one another. The bifurcation diagram is given in in Figure 7.

First, notice from (15) and (20) that the period-one orbits converge to a vertical bouncing orbit at $x = 0$ as H approaches $\frac{g}{2a}$. Recall that the vertical bouncing orbit loses its stability at $H = \frac{g}{2a}$. Hence, one can see that the period-one orbits bifurcate from the vertical bouncing at $x = 0$ when $(H, G) = (\frac{g}{2a}, 0)$.

Second, it follows from (15) and (21) that the period-two orbits bifurcate from the period-one orbits when $(H, G) = (\frac{3g}{2a}, -\frac{g}{2a^2})$.

Third, one can see from (24) that the (vertical bouncing + period-one) orbit at $x_\pm$ in (22) converges to the vertical bouncing orbit at $x = 0$ as G approaches 0 (or, H approaches $\frac{g}{4a}$). Namely, the (vertical bouncing + period-one) orbits bifurcate from the vertical bouncing on $x = 0$ when $(H, G) = (\frac{g}{4a}, 0)$. One can also see from (22) – (24) that

$$\lim_{G \to \frac{g}{2a^2}} x_\pm = \lim_{G \to \frac{g}{2a^2}} \pm\sqrt{\frac{2G}{g}} = \pm\frac{1}{a},$$
$$\lim_{G \to \frac{g}{2a^2}} E(G) = +\infty,$$
$$\lim_{G \to \frac{g}{2a^2}} Q_b = \infty.$$

In other words, as G approaches $\frac{g}{2a^2}$, the (vertical bouncing+ period-one) orbits converge to the orbit in Figure 8.

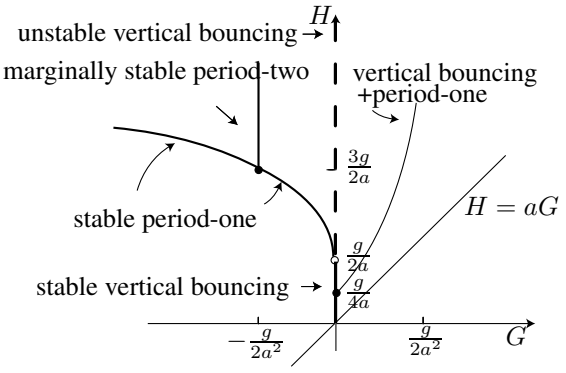

Figure 7. The bifurcation diagram for the four types of periodic orbits: vertical bouncing, period-one, period-two and (vertical bouncing + period-one).

4 Boundary Curvature and Two Stabilization Strategies for Periodic Orbits in the PGB.

We first discuss the role of the curvature of the parabolic boundary of the PGB in stability by comparing it with the flat boundary of the wedge. We then

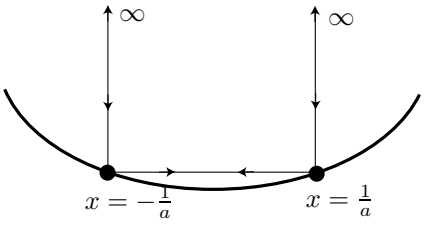

Figure 8. The limit of the (vertical bouncing + period-one) periodic orbit as G approaches $\frac{g}{2a^2}$.

propose two possible strategies for stabilizing periodic orbits: 1. feedback impact control at the boundary and 2. open-loop rotational harmonic vibration of the boundary. These two strategies proved effective with the wedge billiard.

4.1 Boundary Curvature and Stability

Period-two orbits exist in the wedge dynamics only when the wedge is square; see Section 2. In the PGB period-two orbits exist only at $x = \pm\frac{1}{a}$ where the tangent lines at the parabolic boundary have slopes $\pm 45^\circ$. Hence, the period-two orbits in the square wedge billiard also exist in the PGB with appropriate values of a. Even though these orbits have the same shape, they have different stability properties. Recall that period-two orbits are all unstable in the square wedge whereas period-two orbits in the PGB are all Lyapunov stable. One can make the similar observation with the period-one orbits in the wedge and those in the PGB. This indicates that the local curvature of the boundary dictates the stability property of the periodic orbits. The parabolic boundary stabilizes those periodic orbits whereas the flat boundary of the wedge fails to do so except for $\theta < 45^\circ$ with period-one orbits. It follows that in general the (local) curvature shaping of the boundary, if it can be implemented by an additional force, is an effective way of stabilizing periodic orbits.

4.2 Lyapunov-based Feedback Stabilization

We suggest a Lyapunov-based feedback control law to stabilize period-one orbits in the PGB. The main idea is to make use of the conserved quantities H and G – conserved with no control– to identify a period-one orbit and construct a Lyapunov function in terms of (H, G). A similar idea was successfully used for the wedge billiard in [Gerard and Sepulchre, 2004] where the approximated level set of the KAM tori around a period-one orbit was used in place of G as G is not a conserved quantity in the wedge dynamics. This method of constructing Lyapunov functions in terms of conserved quantities was also employed to achieve Lyapunov-based transfer between elliptic Keplerian orbits, [Chang, Chichka and Marsden, 2002].

Recall that the level set in (15) with $H > \frac{g}{2a}$ coincides with the period-one orbit $\{\pm x_H\}$ with x_H in (20). This obervation leads to the following choice of a Lyapunov function:

$$V[k] = (H[k] - H_0)^2 + (G[k] - G_0)^2$$

where k denotes the collision time-sequence and (H_0, G_0) denotes the value of (H, G) at the target period-one orbit; see the bifurcation diagram in Figure 7. We assume that the impact control $u[k]$ is in the direction normal to the boundary. The impact control $\{u[k]\}$ affects $\{H[k]\}$ and $\{G[k]\}$ as follows:

$$H[k] = H[k-1] + u[k](2p_n[k] + u[k]),$$
$$G[k] = G[k-1] - u[k](2p_n[k] + u[k])a(x[k])^2.$$

One needs to choose control $u[k]$ such that

$$\Delta V[k] = V[k] - V[k-1] \leq 0.$$

The performance of this impact feedback control law is being investigated as on-going research.

4.3 Sensorless Stabilization

The idea of stabilizing periodic orbits in impact systems by vibrating the boundary dates back to [Holmes, 1982]. Recently, the stabilization of the period-one and period-two orbits with a rotational harmonic vibration of the wedge in the wedge dynamics was achieved [Ronsse, Lefevre and Sepulchre, 2004]. We summarize this result as follows. First, detect all the period-one and period-two orbits in the wedge dynamics when the collision is elastic, i.e., $e = 1$. Then, consider a real wedge system where the collision is no longer elastic, i.e. $e < 1$. Then, the period-one and period-two orbits, which exist with $e = 1$, will not exist in the case of $e < 1$. One chooses an orbit of interest among them. The question is "can we create, isolate and stabilize this periodic orbit by vibrating the boundary harmonically and rotationally?"; see Figure 9. The answer is yes for the wedge billiard. We expect that the same method will work for the PGB. It is currently under investigation.

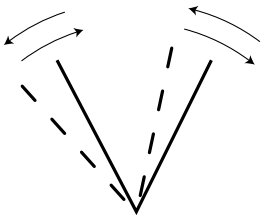

Figure 9. The rotational vibration of the wedge in the harmonic way.

5 Conclusion

This paper suggests two methods for stabilizing periodic orbits in parabolic gravitational billiard (PGB): 1. Lyapunov-based feedback impact control at the boundary and 2. sensorless rotational harmonic vibration of the boundary. Both results proved successful in the case of the wedge billiard, [Ronsse, Lefevre and Sepulchre, 2004; Gerard and Sepulchre, 2004]. Thanks to the local curvature, the bounce juggling in the PGB seems easier than in the wedge billiard.

In this paper, we first reviewed the main properties of the wedge billiard dynamics in Section 2 and then the dynamics of the parabolic gravitational billiard (PGB) in Section 3. The dynamics of the PGB have two conserved quantities: H and G in (1) and (3). By fixing the values of these two quantities, we constructed the reduced Poincaré map and found four different types of periodic orbits. We studied their stability and gave a bifurcation diagram in Figure 7. In Section 4, we emphasized the role of the local curvature of the boundary for stability by comparing the wedge billiard and the PGB. We also proposed two methods for stabilizing periodic orbits in the PGB. As an ongoing work, we are investigating the performance of these methods.

References

Aeyels, D. and Sepulchre, R. [1992] A stability for dynamical systems with first integrals: A topological criterion, *Systems and Control Letters*, **19**, pp. 461–465.

Brogliato, B. (1996). *Nonsmooth Impact Mechanics: Models, Dynamics and Control (Lecture Notes in Control and Information Sciences, 220)*. Springer-Verlag.

Buehler, M., Koditschek, D. and Kindlmann, P. [1994] Planning and control of robotic juggling and catching tasks, *International Journal of Robotics Research*, **13**(2), pp. 101–118.

Chang, D.E., Chichka, D.F. and Marsden, J.E. [2002] Lyapunov-based transfer between elliptic Keplerian orbits, *Discrete and Continuous Dynamical Systems-Series B*, **2**, pp. 57–67.

Gerard, M. and Sepulchre, R. (2004). Stabilization through weak and occasional interactions: a billiard benchmark. In *Proc. IFAC NOLCOS*. Stuttgart, Germany.

Holmes, P. J. [1982] The dynamics of repeated impacts with a sinusoidally vibrating table, *J. Sound Vibration*, **84**(2), pp. 173–189.

Korsch, H. J. and Lang, J. [1991] A new integrable gravitational billiard, *J. Phys. A: Math. Gen.*, **24**, pp. 45–52.

Landau, L.D. and Lifshitz, E.M. (1992). *Mechanics*. Butterworth-Heinemann.

Lehtihet, H.E. and Miller, B.N. [1986] Numerical study of a billiard in a gravitational field, *Phys. D*, **21**(1), pp. 93–104.

Lynch, K.M. and Black, C.K. (1999). Control of underactuated manipulation by real-time nonlinear optimization. In *Proc. 9th international symposium robotics research*.

Ronsse, R., Lefevre, P. and Sepulchre, R. (2004). Open-loop stabilization of 2d impact juggling. In *Proc. IFAC NOLCOS*. Stuttgart, Germany.

Schaal, S. and Atkeson, C.G. (1993). Open loop stable control strategies for robot juggling. In *Proc. IEEE International Conference on Robotics and Automation*, **3**, pp. 913–918.

Sepulchre, R. and Gerard, M. (2003). Stabilization of periodic orbits in a wedge billiard. In *Proc. 42nd IEEE CDC*. Hawaii.